

Coupling the MULTI-VP model with EUHFORIA

E. Samara^{1,2}, R. F. Pinto^{3,4}, J. Magdalenic¹, V. Jercic², C. Scolini²,
L. Rodriguez¹, S. Poedts²

¹Royal Observatory of Belgium, Brussels, Belgium

²Centre for mathematical Plasma Astrophysics, KU Leuven, Leuven, Belgium

³IRAP, Université de Toulouse, CNRS, UPS, CNES, Toulouse, France

⁴LDE3, CEA Saclay, Université Paris-Saclay, Gif-sur-Yvette, France

Online EGU General Assembly 2020

ST1.8 - Winds of change: New perspectives on the properties of solar
transients throughout the heliosphere

Outline

Introduction

- EUHFORIA and its default set-up
- The MULTI-VP model
- Why implementing the MULTI-VP model into EUHFORIA is important
- Main differences between the default coronal model in EUHFORIA and MULTI-VP

Inner Boundary (0.1 AU):

the transition from the coronal to the inner heliospheric modeling domain

- Corrections for subalfvenic speeds at 0.1 AU
- Comparison between MULTI-VP and WSA output with GONG synoptic magnetograms
- Comparison between MULTI-VP and WSA output with WSO synoptic magnetograms

High speed stream signatures at 1 AU:

- Comparison between MULTI-VP+EUHFORIA and WSA+EUHFORIA time series at Earth

2-case study:

one high-speed stream event during solar minimum and one during solar maximum activity, respectively

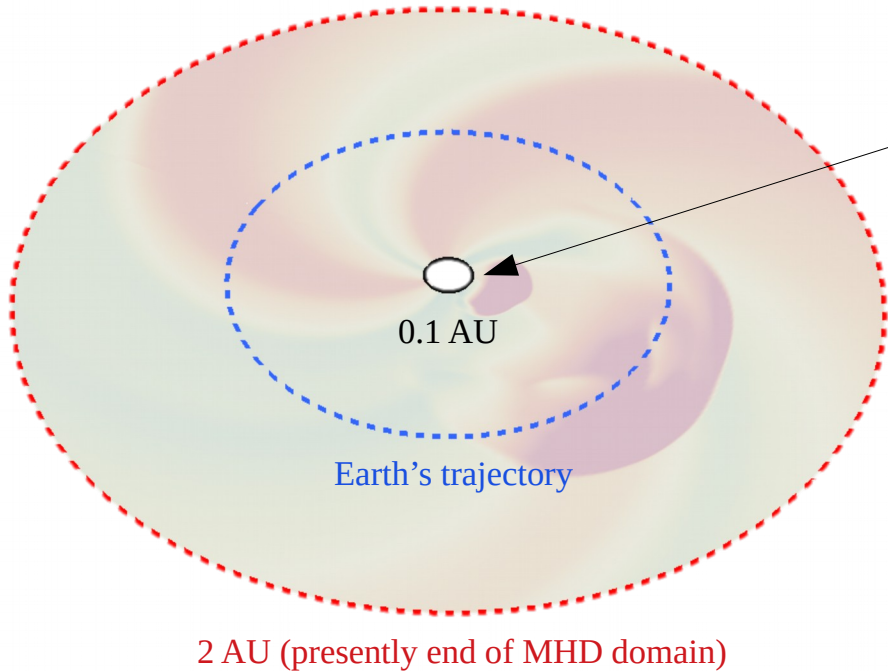
Summary & Conclusions



coronal model + inner heliosphere model

1. EUHFORIA and its default set-up

(Pomoell & Poedts, 2018)



- Default coronal model (until 0.1 AU):
 - Wang-Sheeley-Arge (WSA) semi-empirical model in combination with the PFSS and Schatten Current Sheet (SCS) model.
 - The coronal model produces the necessary boundary conditions that are later used as input to the inner heliospheric part of EUHFORIA.
- CMEs insertion at 0.1 AU
- Inner heliosphere (0.1 AU – 2 AU):
 - 3D MHD time-dependent simulation of CMEs and steady-state propagation of solar wind.

Fig. 1: Equatorial plane of EUHFORIA's complete domain. The black solid circle indicates the inner boundary (0.1 AU) beyond which the inner heliospheric part of EUHFORIA initiates. *Image credits: Jens Pomoell.*



coronal model + inner heliosphere model

1. EUHFORIA and its default set-up

(Pomoell & Poedts, 2018)

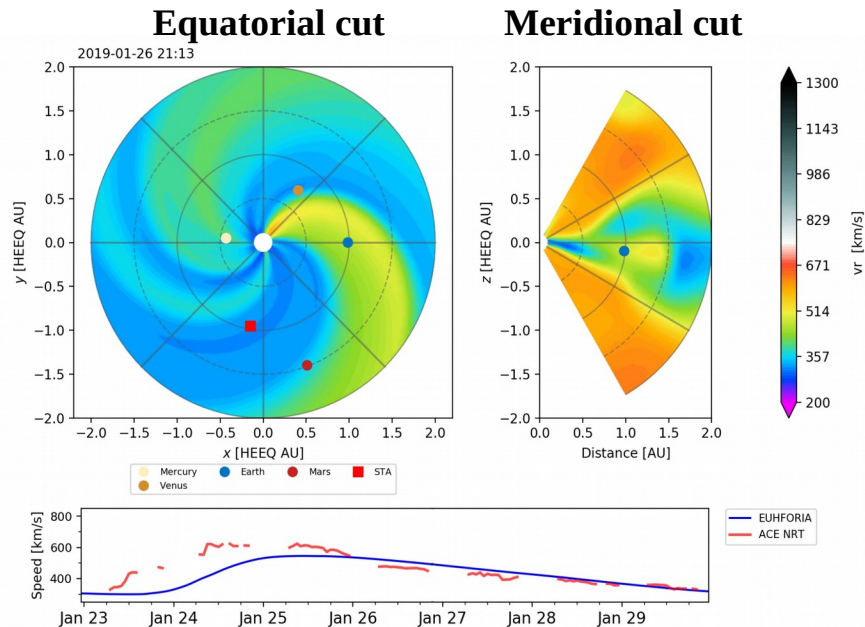


Fig. 2: Equatorial (upper left) and meridional (upper right) cut of EUHFORIA's output, modeling a high-speed stream (HSS) that reached Earth on 2019-01-23. The magnitude of the solar wind radial velocity is color coded. The lower panel shows the HSS radial velocity signature at Earth as given by ACE satellite data (red) and EUHFORIA output (blue).

- Default coronal model (until 0.1 AU):
 - Wang-Sheeley-Arge (WSA) semi-empirical model in combination with the PFSS and Schatten Current Sheet (SCS) model.
 - The coronal model produces the necessary boundary conditions that are later used as input to the inner heliospheric part of EUHFORIA.
- CMEs insertion at 0.1 AU
- Inner heliosphere (0.1 AU – 2 AU):
 - 3D MHD time-dependent simulation of CMEs and steady-state propagation of solar wind.

2. The MULTI-VP coronal model

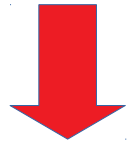


- Physics-based model (output at 0.1 AU are produced after solving a set of MHD equations).
- Magnetograms are used as the first source of information; the coronal magnetic field is reconstructed by employing PFSS extrapolations.
- The numerical code solves the system of MHD equations describing the heating and acceleration of a wind stream along a given magnetic flux-tube. Every such flux tube is a 1D wind solution. Eventually, the total of all these 1D solutions sample the whole solar atmosphere.

Fig. 3: The grey scale in solar surface indicates the input WSO magnetogram in the MULTI-VP model for CR2056 (2007 April–May). A sample of magnetic field lines obtained via PFSS extrapolation used to initiate the model, are also depicted. The transparent yellow surface indicates the coronal hole boundaries (closed-field regions are excluded from the domain). For more details see *Pinto & Rouillard, 2017*.

3. Why implementing the MULTI-VP model into EUHFORIA is important

- Results of solar wind modeling by employing the default EUHFORIA set up (from now on, **WSA-EUHFORIA**) often overestimate or underestimate the high speed stream (HSS) signatures and the background solar wind (*see Hinterreiter et al., 2018*).
- Without a proper modeled solar wind, modeling of CMEs is also not trustworthy for reliable space weather forecasting.



Implementation and testing of different coronal models in EUHFORIA is essential towards achieving the set up which will result in optimal modeled output and thus, the most accurate space weather predictions!

4. Main differences between the default coronal model in EUHFORIA and MULTI-VP

Default coronal model in EUHFORIA**

- It uses the WSA model, which is a **semi-empirical model**. The solar wind speed v , is the quantity around which the model is built and is obtained through a function of the flux tube expansion factor and the distance from the coronal hole boundary, which are both properties of the magnetic field. Once the velocity is calculated, all other quantities (n , T , B_r) are estimated at 0.1 AU as a function of it.
- Uses the **PFSS** and **Schatten Current Sheet (SCS)** models. The latter specifically contributes for the radial extension of the magnetic field while retaining a thin structure for the heliospheric current sheet.
- The source surface height for the PFSS extrapolations is set at $r=2.6 R_{\text{sun}}$.

MULTI-VP

- **Physical model**. It solves a set of MHD equations to provide output at 0.1 AU.
- Uses the **PFSS** but not the **SCS** model. Nevertheless, the **SCS's** job is done by letting the expansion profile of the streams re-adjust in the high corona such that the interplanetary magnetic field becomes more uniformly distributed, transverse pressure balance can be achieved and density scales correctly with wind speed (for more information, see *Pinto & Rouillard, 2017*).
- The source surface height for the PFSS extrapolations is set at $r=2.5 R_{\text{sun}}$.

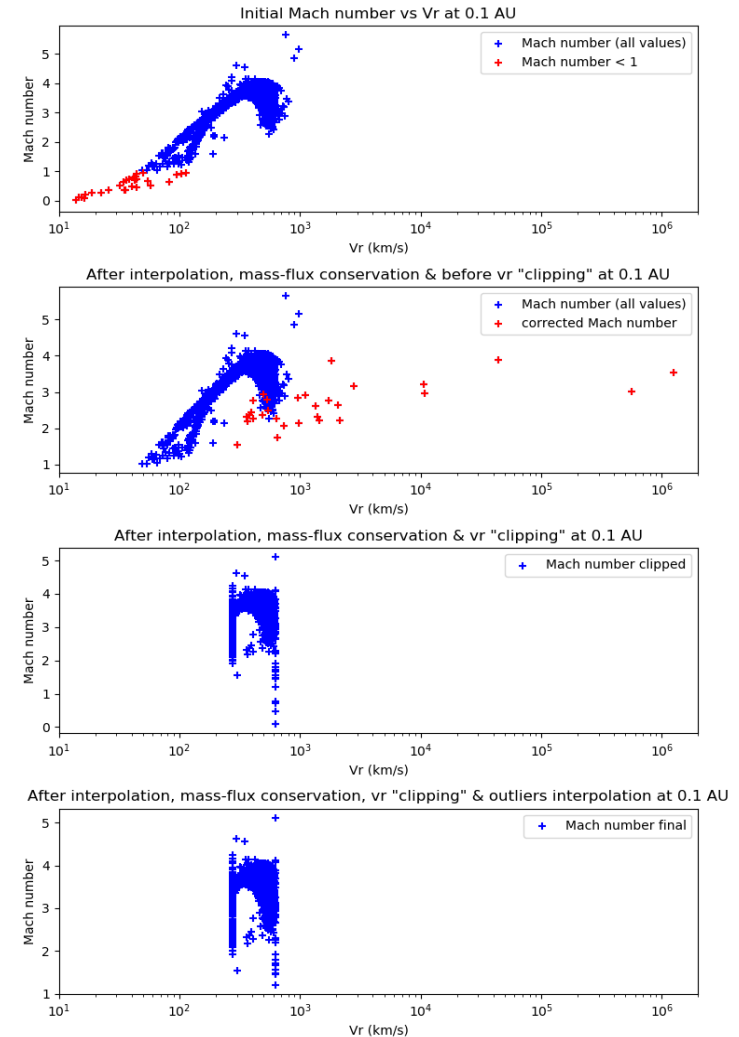
** From this point on and for brevity reasons, we will call the “default coronal model in EUHFORIA” as “WSA” model, keeping in mind that the latter is used in combination with the PFSS+SCS models.

Inner Boundary (0.1 AU):

the transition from the coronal to the inner heliospheric modeling domain

- **Corrections for sub-alfvenic speeds at 0.1 AU**
- Before inserting the MULTI-VP data into the MHD part of EUHFORIA, **we need to make sure that all values are super-alfvenic at the boundary.** The inner heliospheric part of EUHFORIA **does not accept** sub-alfvenic values !
- In case sub-alfvenic values are found :
 1. All pixels characterized by a Mach number (M) < 1 are interpolated with their first, super-alfvenic neighbors.
 2. Based on the new Mach numbers, we calculate the new radial velocity (v_r) & density (n) at the boundary by conserving the mass-flux (see panel 2 of Fig. 4).
 3. Restricting v_r between [275, 625] km/s (as done by default in EUHFORIA, see *Pomoell & Poedts, 2018* and panel 3 of Fig. 4) and employing again the mass-flux conservation to calculate the new n , can occasionally lead to a few pixels with $M < 1$. These are assumed as “outliers” and are interpolated for one last time (see panel 4 in Fig. 4).

Fig. 4: Mach number as a function of radial velocity at 0.1 AU. The different panels indicate the steps followed to correct the sub-alfvenic values from the MULTI-VP model before inserting them into the heliospheric part of EUHFORIA.





➤ **MULTI-VP vs WSA output at 0.1 AU with GONG synoptic magnetograms**

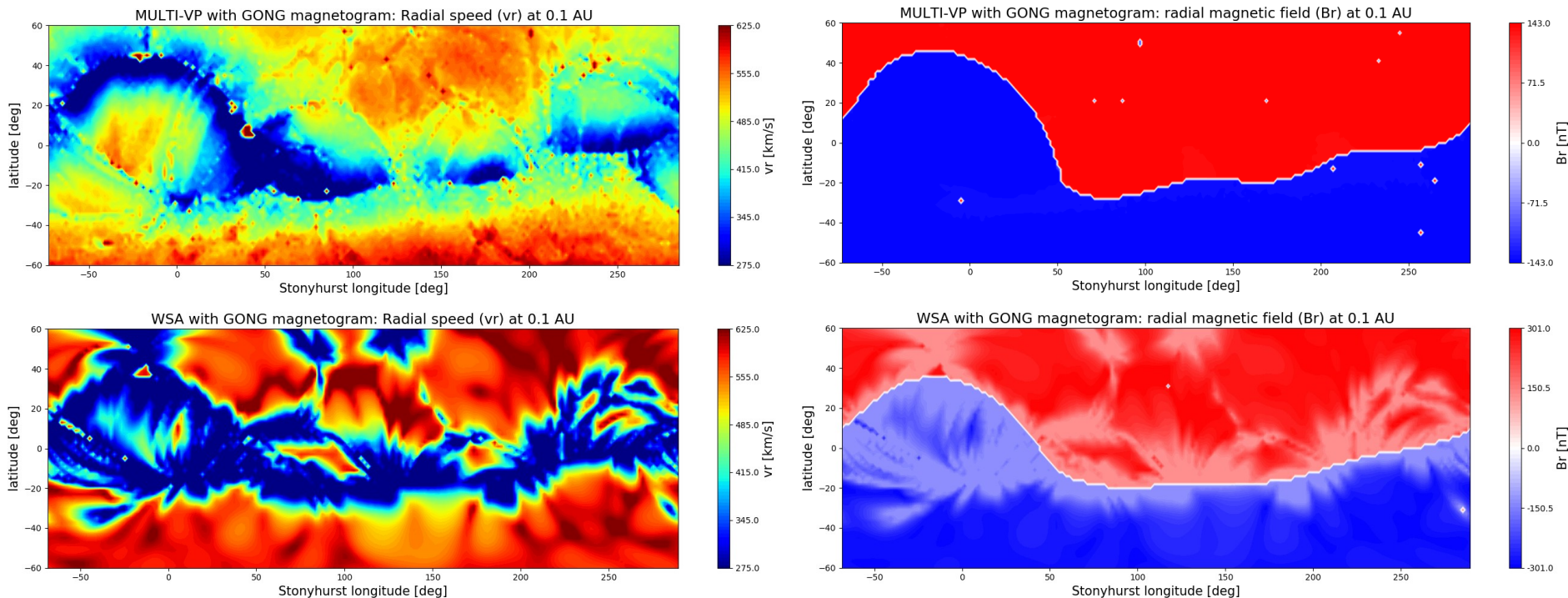


Fig. 5: 2D maps of radial velocity, v_r , (left column) and radial magnetic field, Br , (right column) at 0.1 AU as produced by the daily updated GONG synoptic magnetogram on 2018-01-17T23:14. The first row shows output based on the MULTI-VP model while the second row on the WSA model. The upper left panel is the final result after the correction of 30 sub-alfvenic values over the total of 16200 values at the boundary. Furthermore, a faster solar wind stream seems to emerge from the coronal hole located between $\sim[-50^\circ-0^\circ]$ in longitude on the MULTI-VP v_r map, compared to the WSA v_r map.



➤ **MULTI-VP vs WSA output at 0.1 AU with GONG synoptic magnetograms**

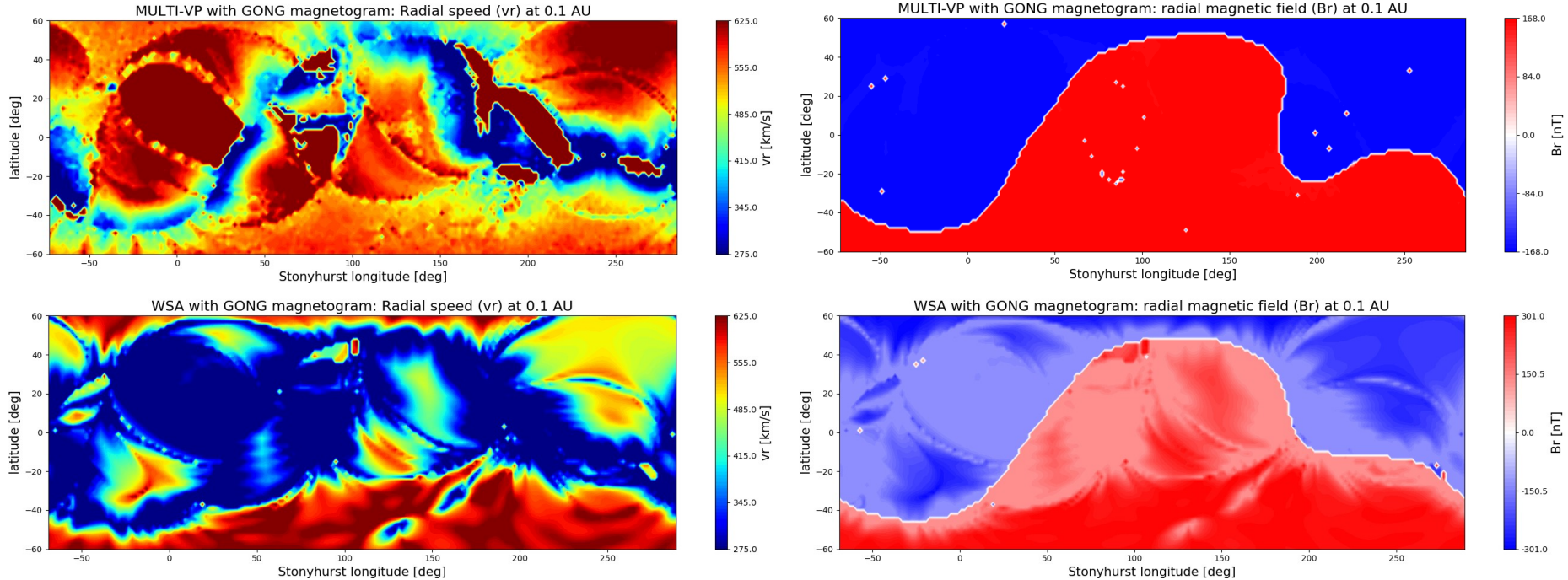


Fig. 6: 2D maps of radial velocity, v_r , (left column) and radial magnetic field, Br , (right column) at 0.1 AU as produced by the daily updated GONG synoptic magnetogram on 2011-06-20T23:54. The first row indicates output based on the MULTI-VP model while the second row on the WSA model. The upper left panel is the final result after the correction of 1196 sub-alfvenic values over the total of 16200 values at the boundary. The ellipsoidal region extending between $[-50^\circ, 50^\circ]$ in longitude together with a part of the region extending between $[150^\circ, 250^\circ]$ in longitude at both v_r maps, are complicated areas that seem to be characterized by very low speeds in both the WSA and MULTI-VP case (before the applied sub-alfvenic corrections). Nevertheless, after these corrections in the MULTI-VP data, the aforementioned regions turn to fast solar wind areas as they are surrounded by high-speed neighbors. Moreover, the area of the coronal hole from which the HSS of interest originated (situated between $[-40^\circ, 0^\circ]$ in latitude and $[-50^\circ, 0^\circ]$ in longitude), seems well captured by both models.



➤ **MULTI-VP vs WSA output at 0.1 AU with WSO synoptic magnetograms**

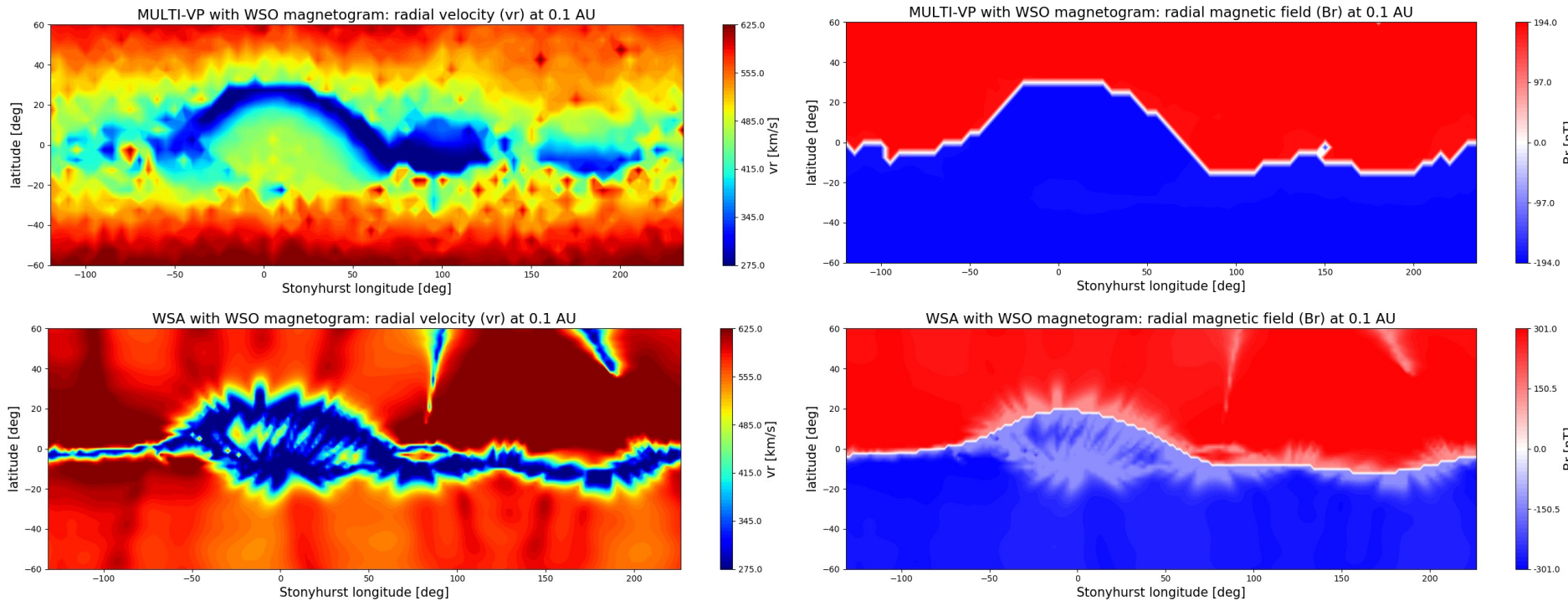


Fig. 7: 2D maps of radial velocity, v_r , (left column) and radial magnetic field, B_r , (right column) at 0.1 AU as produced by the WSO synoptic magnetogram of Carrington Rotation CR2199. CR2199 includes the day of interest (2018-01-17T23:14) so it was the only map we could use to reproduce the HSS of interest. The first row indicates output based on the MULTI-VP model while the second row on the WSA model. There were no sub-alfvenic velocities for this case.



➤ **MULTI-VP vs WSA output at 0.1 AU with WSO synoptic magnetograms**

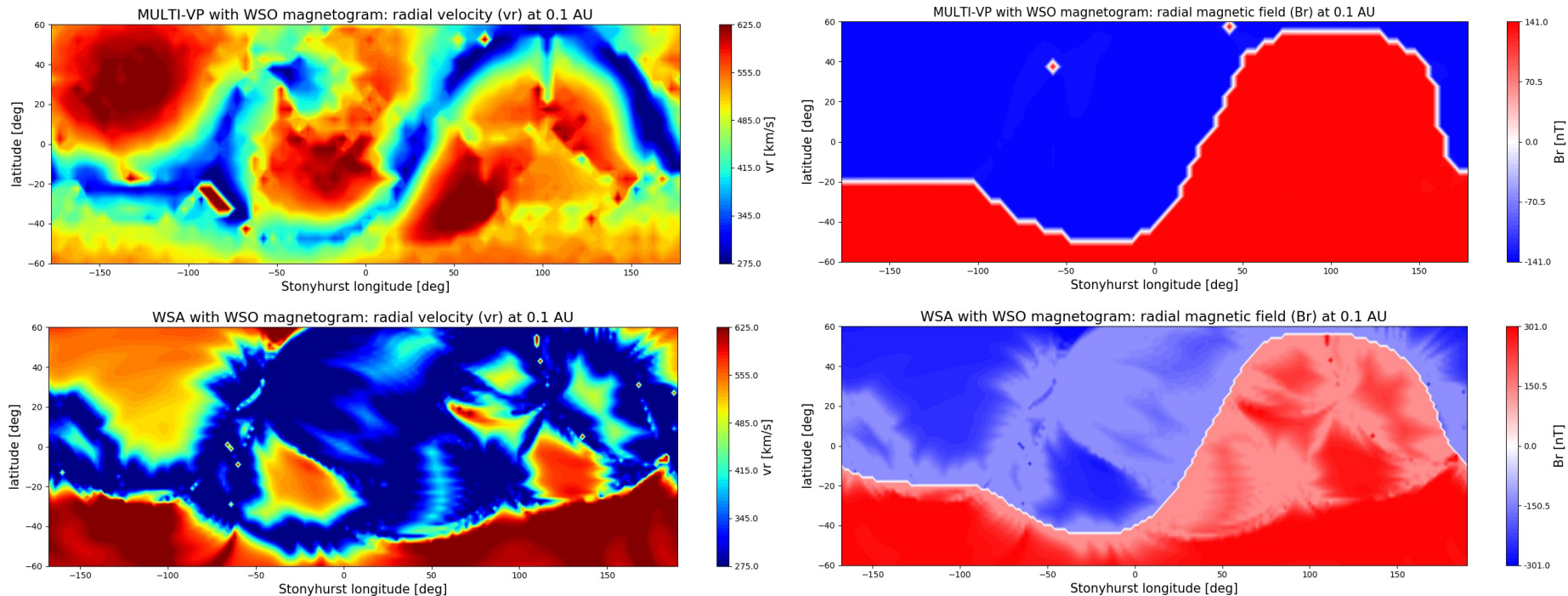


Fig. 8: 2D maps of radial velocity, v_r , (left column) and radial magnetic field, Br , (right column) at 0.1 AU as produced by the WSO synoptic magnetogram of Carrington Rotation CR2111. CR2111 includes the day of interest (2011-06-20T23:54) so it was the only map we could use to reproduce the HSS of interest. The first row indicates output based on the MULTI-VP model while the second row on the WSA model. The upper left panel is the final result after the correction of 7 subalfvenic values over the total of 2592 values at the boundary. This time we distinguish an extended area of slow solar wind given by WSA between $[-50^\circ, 100^\circ]$ in longitude (lower left map) which is not present in the MULTI-VP output (upper left panel).

Runs conducted with GONG magnetogram of 2018-01-17T23:14

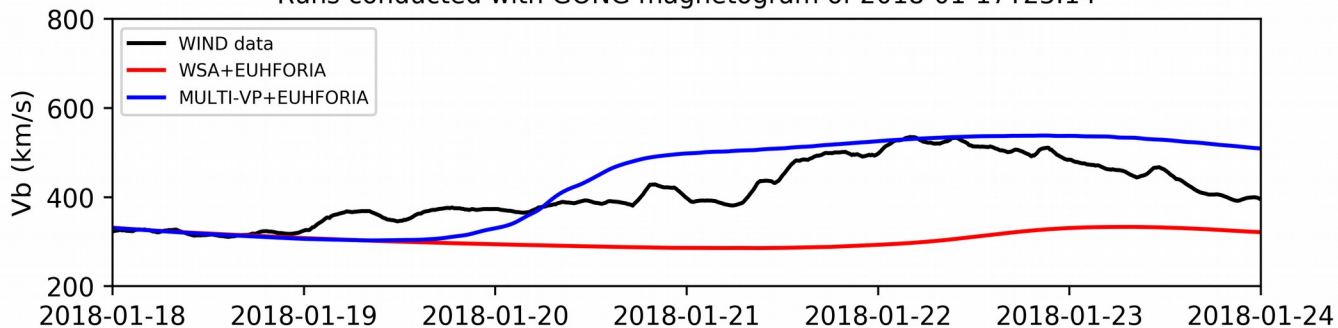
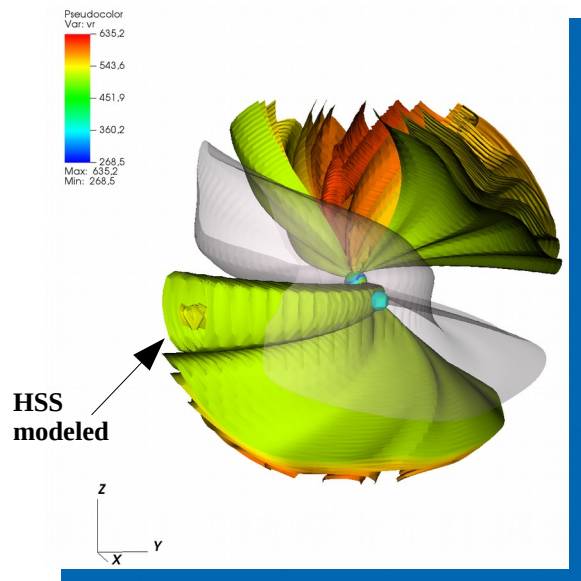


Fig. 9: HSS bulk speed at Earth as modeled by WSA+EUHFORIA (red) and MULTI-VP+EUHFORIA (blue) for 6 days of forecasting. Both runs have been conducted with the GONG synoptic magnetogram taken on 2018-01-17T23:14. The MULTI-VP+EUHFORIA output captures the real HSS while this is not the case for the WSA+EUHFORIA.

MULTI-VP+EUHFORIA



WSA+EUHFORIA

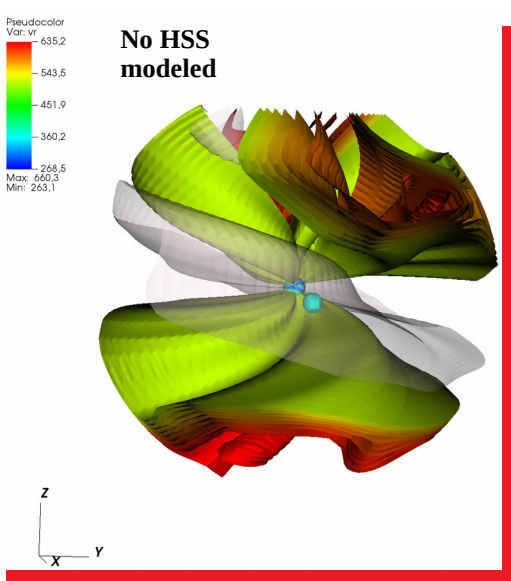


Fig. 10: 3D visualizations of the structures produced by WSA+EUHFORIA and MULTI-VP+EUHFORIA throughout the inner heliospheric domain. The heliospheric current sheet is indicated in grey while the colorful isosurfaces represent solar wind speeds between 520 and 600 km/s. A demonstration of the spherical inner boundary surface can be seen in the middle of the domain. It depicts the radial velocities at 0.1 AU. Earth is shown in light blue color.

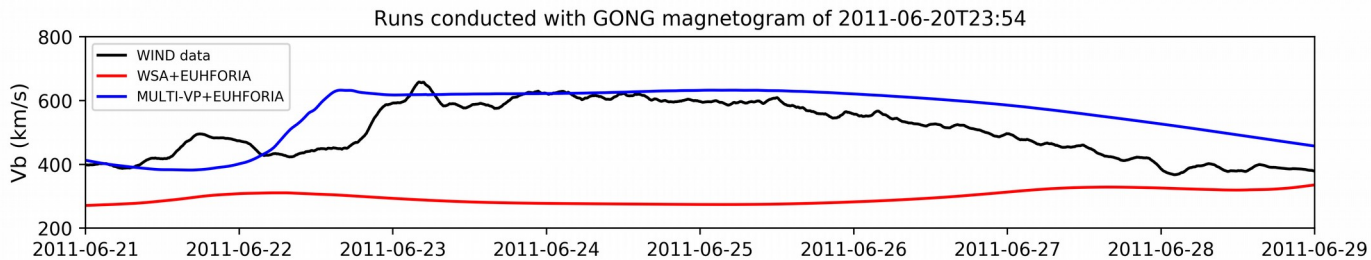


Fig. 11: HSS bulk speed at Earth as modeled by WSA+EUHFORIA (red) and MULTI-VP+EUHFORIA (blue) for 8 days of forecasting. Both runs have been conducted with the GONG synoptic magnetogram taken on 2011-06-20T23:54. The MULTI-VP+EUHFORIA output reproduces the real HSS detected at Earth while this is not the case for the WSA+EUHFORIA.

MULTI-VP+EUHFORIA

MULTI-VP+EUHFORIA

WSA+EUHFORIA

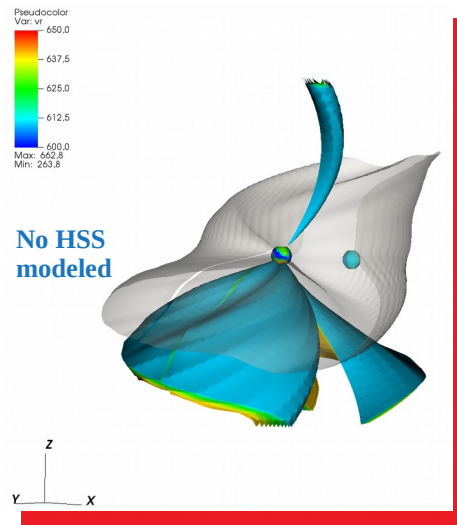
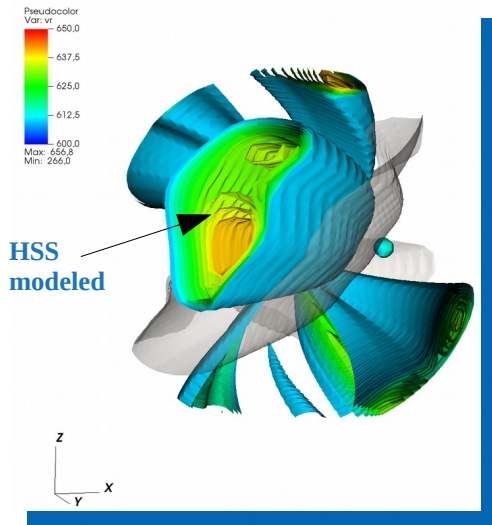
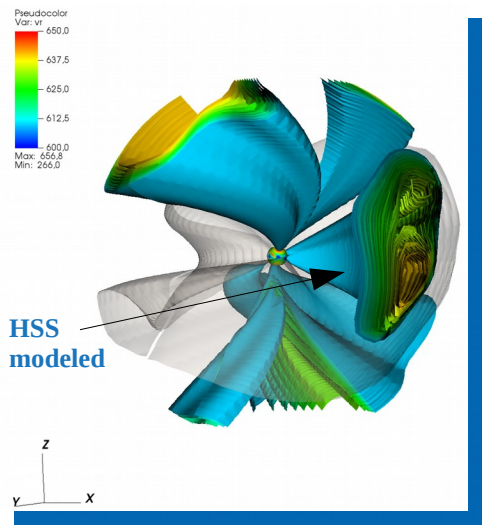


Fig. 12: 3D visualizations of the structures produced by WSA+EUHFORIA and MULTI-VP+EUHFORIA throughout the inner heliospheric domain. Same description applies as in Fig. 10 but the range of the colorful isosurfaces now range between 600 km/s and 650 km/s.

Solar minimum case

(WSO magnetogram of CR2199, for the same solar minimum case as presented in slide 13)

High speed stream signatures at 1 AU

Runs conducted with WSO magnetogram of CR2199

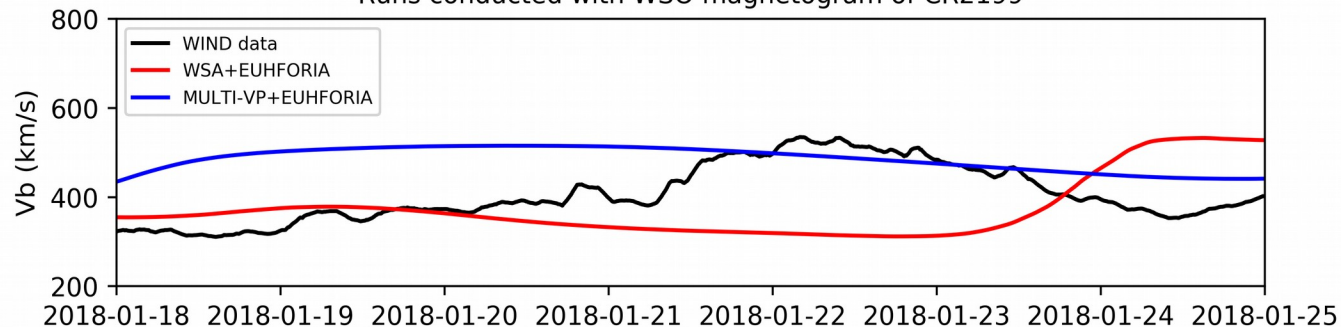
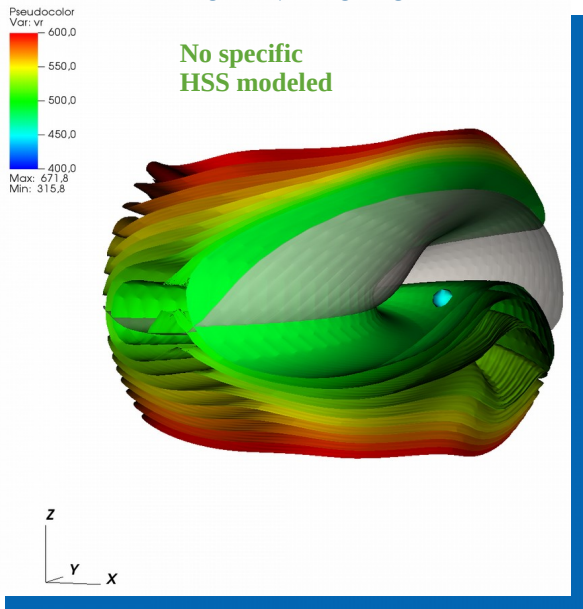


Fig. 13: HSS bulk speed at Earth as modeled by WSA+EUHFORIA (red) and MULTI-VP+EUHFORIA (blue) for 6 days of forecasting. Both runs have been conducted with the WSO synoptic magnetogram of CR2199. None of the aforementioned time series performs well regarding the arrival of the real HSS.

MULTI-VP+EUHFORIA



WSA+EUHFORIA

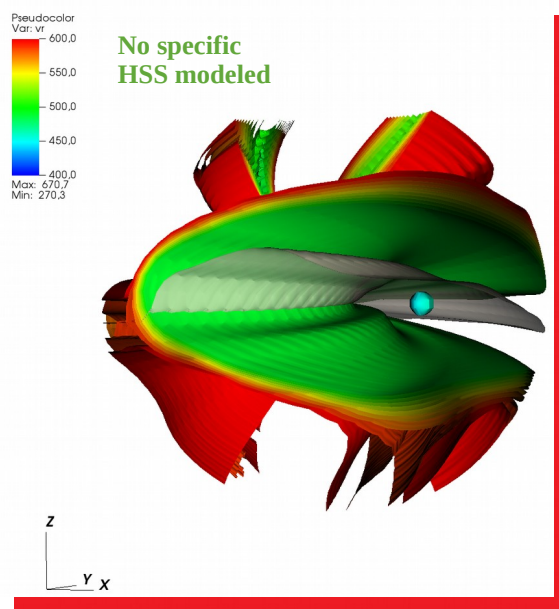


Fig. 14: 3D visualizations of the structures produced by WSA+EUHFORIA and MULTI-VP+EUHFORIA throughout the inner heliospheric domain. Same description applies as in Fig. 10 and 12, but the range of the colorful isosurfaces now range between 500 km/s and 600 km/s.

Solar maximum case

(WSO magnetogram of CR2111, for the same solar maximum case as presented in slide 14)

High speed stream signatures at 1 AU

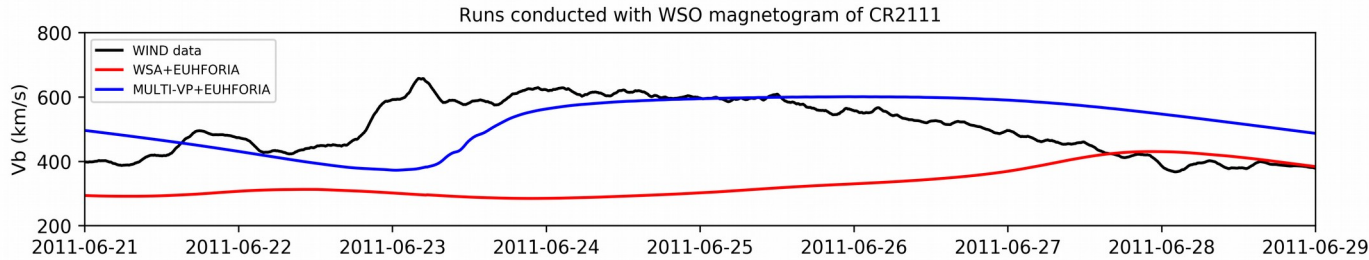


Fig. 15: HSS bulk speed at Earth as modeled by WSA+EUHFORIA (red) and MULTI-VP+EUHFORIA (blue) for 8 days of forecasting. Both runs have been conducted with the WSO synoptic magnetogram of CR2111. The MULTI-VP+EUHFORIA output captures the real HSS while this is not the case for the WSA+EUHFORIA output.

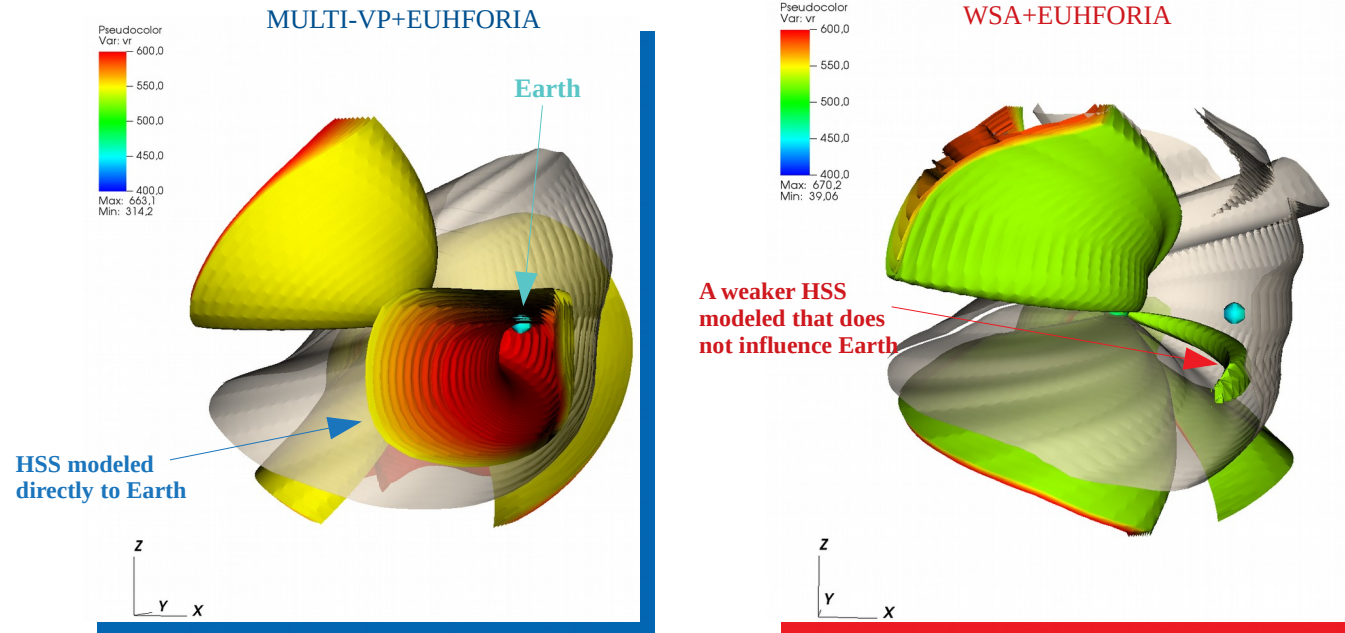


Fig. 16: 3D visualizations of the structures produced by WSA+EUHFORIA and MULTI-VP+EUHFORIA throughout the inner heliospheric domain. Same description applies as in Fig. 10, 12 and 14 but the range of the colorful isosurfaces now range between 490 km/s and 600 km/s.

- In this work, we implemented and tested a different coronal model in EUHFORIA, the so-called **MULTI-VP** model (*Pinto & Rouillard, 2017*). The obtained results, both at inner boundary (0.1 AU) and at 1 AU, were compared to the default set up of **EUHFORIA (WSA+EUHFORIA)**.
- Two high-speed stream (HSS) cases are tested; one during the solar minimum and one during the solar maximum activity of the Sun. Comparison between **WSA+EUHFORIA** and **MULTI-VP+EUHFORIA** is conducted by using:
 - (a) the same GONG synoptic magnetogram (one for the solar minimum and one for the solar maximum case) and
 - (b) the same WSO magnetogram (one for the solar minimum and one for the solar maximum case).
- We further present how the smooth implementation of the **MULTI-VP** data in the inner heliospheric part of **EUHFORIA** is done, in case sub-alfvenic speeds are detected at the boundary.

Results:

- A number of qualitative and quantitative differences are observed in the v_r and B_r 2D maps at 0.1 AU between the **MULTI-VP** and **WSA** coronal models, when using the same magnetogram. This is to be expected because of the nature of the two models (physics-based and semi-empirical, respectively). A major difference can be specifically located in all B_r maps, at which we distinguish a gradient in B_r values estimated by the **WSA** model. This gradient comes from the fact that the radial magnetic field at 0.1 AU is calculated as a function of the empirical velocity (see slide 7), based on the following relation:

$$B_r = \text{sgn}(B_{\text{corona}})B_{\text{fsw}}(v_r/v_{\text{fsw}})$$

where $\text{sgn}(B_{\text{corona}})$ is the sign of the magnetic field as given by the coronal model, v_r is the empirical solar wind speed at 0.1 AU and $v_{\text{fsw}} = 675$ km/s refers to the speed of the fast solar wind that carries a magnetic field of $B_{\text{fsw}} = 300$ nT (see *Pomoell & Poedts, 2018* for more details). On the other hand, the **MULTI-VP** B_r maps are not characterized by any kind of gradient; they are uniform and converge to either a positive or a negative B_r value. This is because, after the PFSS extrapolations, an additional flux-tube expansion profile is applied to smoothly transform the very non-uniform field at the source surface, into a uniform field.

- Besides the difference in our results due to the nature of the two coronal models, differences imposed by different magnetograms should also be accounted for. Magnetograms are constructed based on a variety of techniques depending on the observatory that provides them (see *Riley, P. et al., 2014*); thus, differences in our results (in the frame of a specific coronal model), should also be expected because of them.
 - The **MULTI-VP+EUHFORIA** modeled output, based on the GONG magnetograms, successfully captured the two HSSs that reached Earth; Nevertheless, **WSA+EUHFORIA** failed to reproduce the fast solar wind streams of interest, when using exactly the same magnetograms.
 - The **MULTI-VP+EUHFORIA** modeled output, based on the WSO magnetograms, captured well the HSS event during the solar maximum activity. For the solar minimum case though, **MULTI-VP+EUHFORIA** provided continuously overestimated time series which cannot be assumed as successful reproduction of the real event. For the latter case, **WSA+EUHFORIA** output seems to detect a HSS event 3 days later than expected. Its not certain if the increase in bulk speed concerns the HSS of interest or the HSS detected later.
- Regarding the solar maximum case, **WSA+EUHFORIA** also didn't capture the event.

Summary & Conclusions

Future steps:

- Analysis of the rest of the plasma (n , T) and magnetic field parameters (B_x , B_y , B_z , where applicable) at 0.1 AU and 1 AU, respectively
- Increase of the statistics (test more HSS cases with **MULTI-VP+EUHFORIA** and **WSA+EUHFORIA**)
- Understanding the differences that arise (a) because of the different coronal models and (b) because of the different magnetograms
- Quantification of the performance of the modeled output at Earth

Acknowledgments:

The authors would like to acknowledge Jens Pomoell, from the University of Helsinki, for his instructive advice on this work, as well as Immanuel C. Jebaraj, from the Royal Observatory of Brussels, for his enlightening instructions on the visualization procedures.

References:

- Hinterreiter J. et al., *Solar Physics*, Vol. 294, 2019
- Pinto R. and Rouillard A., *The Astrophysical Journal*, Vol. 838, 2017
- Pomoell J. and Poedts S., *Journal of Space Weather & Space Climate*, Vol. 8, 2018
- Riley, P. et al., *Solar Physics*, Vol. 289, 2014

(Next slide shows the magnetograms used in this work) 19

Magnetograms used in this work

